Lawrence Berkeley Laboratory

UNIVERSITY OF CALIFORNIA

Accelerator & Fusion Research Division

A HIGH CURRENT HEAVY ION BEAM TRANSPORT
EXPERIMENT AT LBL

W. Chupp, A. Faltens, E.C. Hartwig, D. Keefe,
C.H. Kim, C. Pike, S.S. Rosenblum, M. Tiefenback,
D. Vanecek, and A.I. Warwick

January 1984

A HIGH CURRENT HEAVY ION BEAM TRANSPORT EXPERIMENT AT LBL*

W. Chupp, A. Faltens, E. C. Hartwig, D. Keefe, C. H. Kim, C. Pike,
S. S. Rosenblum, M. Tiefenback, D. Vanecek, and A. I. Warwick
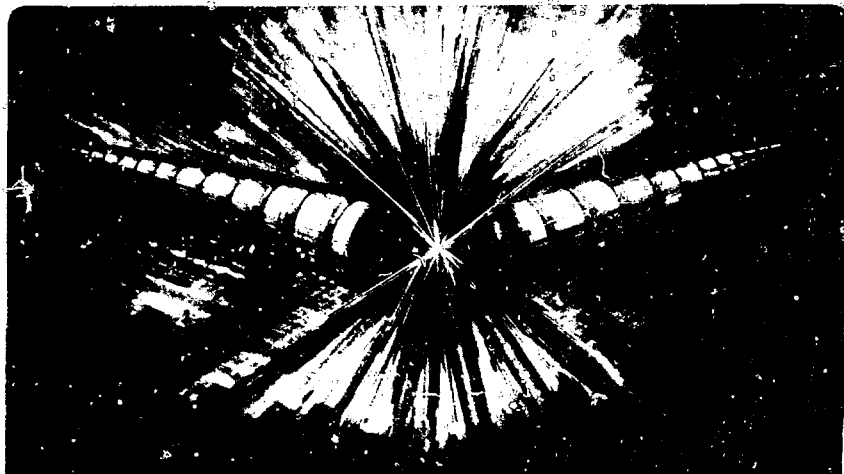

Lawrence Berkeley Laboratory
University of California
Berkeley, California 94720

January 1984

DISCLAIMER

A HIGH CURRENT HEAVY ION BEAM TRANSPORT EXPERIMENT AT LBL*

W. Chupp, A. Faltens, E. C. Hartwig, D. Keefe, C. H. Kim, C. Pike,
S. S. Rosenblum, M. Tiefenback, D. Vanecek, and A.I. Warwick

Lawrence Berkeley Laboratory
University of California
Berkeley, California

Introduction

Information on the current limit in a long quadrupole transport channel
is required in designing an accelerator driver for an inertial confinement
fusion system.[1] Although a current transport limit was proposed by
Maschke,[2] quantitative estimates require a detailed knowledge of the sta-
bility of the beam. Analytic calculations based on the Kapchinskij-
Vladimirskij (K-V) distribution function have identified transversely
unstable modes, but particle simulations[3] have shown that some of the K-V
instabilities are benign, i.e., particles redistribute themselves in the 4-D
transverse phase space, but the rms emittances do not grow. Some
preliminary results of beam transport experiments were reported in the 1983
Particle Accelerator Conference in Santa Fe.[4,5,6,7]

In the "smooth approximation", particles in a quadrupole focussing
channel execute simple harmonic motions whose frequency (ω_β) is given by

$$\omega_\beta^2 = \omega_{\beta 0}^2 - \frac{1}{2}\,\omega_p^2 \tag{1}$$

where symbols from left denote the betatron frequencies with and without the
space charge and the beam plasma frequency, $(4\pi n e^2/M)^{1/2}$. Eq. (1) can
be rewritten in terms of the beam current density (j) and the phase advances
of the betatron oscillation per lattice period (2L) with and without the
space charge (σ and σ_0 respectively);

$$j = 3.75\times10^{-11}\ A^{-1/2}\ L^{-2}\ (\sigma_0^2 - \sigma^2)\ T^{3/2}$$

where A is the atomic mass number, T the kinetic energy in eV, σ's in degrees and j and L are in mks units. Eq. (2) agrees very well with the K-V calculation for $\sigma_0 = 60°$ (see fig. 4). The K-V envelope equation shows that the beam cross-section scales as ϵ/σ for $\sigma/\sigma_0 \ll 1$ where ϵ is the unnormalized beam emittance. The benefits of operating the transport channel at small σ values are obvious. Maschke's original assumption was $(\sigma/\sigma_0)^2 \geq 0.5$, and the value used in the earlier driver designs based on the K-V stability calculation was $\sigma/\sigma_0 \geq 0.4$.

Experimentally, we define stable propagation of the beam if the beam current, size, and emittance measured at the end of the transport channel (41 lattice periods) are the same as the values measured at the beginning. We find that:

1. Stable beam transport is observed for $\sigma_0 = 60°$ and $\sigma \geq 12°$

2. Strong instabilities are observed for $\sigma_0 = 120°$ and $\sigma \leq 90°$

3. The semi-gaussian nature of the particle distribution (i.e., uniform in configuration space, gaussian in transverse velocity space) is approximately preserved for $\sigma_0 = 60°$ and $\sigma/\sigma_0 \approx 0.2$.

Apparatus

The apparatus (Fig. 1) consists of the ion source, injector (gun), matching section (5 quadrupoles M1-M5), transport section (82 electrostatic quadrupoles Q1-Q82), and the diagnostic tank. The fact that a beam is stable in a channel of 82 quadrupoles does not insure that the beam will be stable in a longer channel such as in the ICF driver which may have a few hundred periods and includes acceleration. However, we believe that the present experiment can provide necessary conditions for the beam stability and can serve as an incentive to develop more accurat computational techniques. A more complete description of the apparatus can be found in our earlier publication.[4] Because of the high voltages on the electrostatic quadrupoles, the placement of diagnostics is restricted to the mid-plane between any pair of quadrupoles. At such a location – the antisymmetrical

point of the lattice – the phase ellipses in the xx' and yy' planes for a matched beam are similar in shape but tilted with equal and opposite angles (astigmatic). The ranges of the Cs^+ beam parameters and the ways they are varied are listed below.

> Kinetic energy (T): 80 – 160 keV (Marx Generator)
> Beam Current (I): 0.7 – 23 mA (Current Attenuators)
> Beam Emittance (ϵ_N): 0.8 – 5 x 10^{-7} π Rad m (Biased Grids)

The current is measured with a gridless deep Faraday cup (with an uncertainty of ±2%) at the end of the transport section and with a shallow gridded Faraday cup (0 to –10%) in between quadrupoles at the end of the matching section. The kinetic energy is measured by the time of flight method (±2%). The beam emittance is measured by a two slit scan method (±10%), using two 0.25 mm slits separated by one lattice half–period (15.24 mm) followed by a shallow Faraday cup. The beam current profile is measured with a single slit and a shallow Faraday Cup, or with a "harp" which consists of a 32 isolated parallel wires spaced 1.25 mm apart. The beam radii (a and b for horizontal and vertical, respectively) are deduced from the measured profiles by the rms analysis, and the tilts (a' and b') from the emittance plots. For a perfectly matched beam, a = b, and a' = –b' at the antisymmetry points.

The particle distribution function at the end of the injector is semi-Gaussian. The semi–Gaussian distribution gives an elliptical current profile just as a K–V distribution would. The measured beam emittance is approximately five times higher than expected from the thermal temperature of the zeolite ion source (0.1 eV). We believe that the non–uniformity of the ion emission from the source and the presence of the grid(s) between the injector and the matching section are responsible for the observed higher temperature.

Experimental Procedure

Beam matching and data analysis are guided by the rms envelope equation derived by Sacherer.[8] The rms emittance is defined as

$$\epsilon_{rms} = (\beta\gamma)\sqrt{\langle x^2 \rangle \langle x'^2 \rangle - \langle xx' \rangle^2}$$

DIAGNOSTIC SECTION   TRANSPORT SECTION   MATCHING SECTION   SOURCE
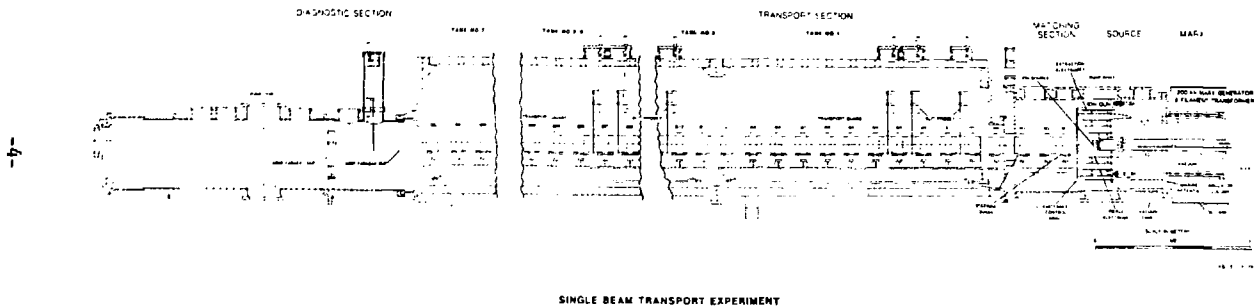
SINGLE BEAM TRANSPORT EXPERIMENT

Fig. 1.   Schematic diagram of the apparatus showing (from right to left) the ion source, gun (injector), matching section (5 quadrupoles M1–M5) , transport section (82 quadrupoles Q1–Q82) and the diagnostic section. Ranges of beam parameters are listed in the text. Lattice-half period = 15.24 cm, bore diameter = 5.08 cm.

where $\beta\gamma$ are the usual relativistic parameters and the brackets denote averaging over the distribution function. Values of σ_0 and σ are calculated from the equivalent K-V beam which has the same current, has $\epsilon_N = 4\epsilon_{rms}$, and has a beam radius $a = 2 x_{rms}$. For the desired values of σ_0 and σ, we adjust the injector and lattice parameters (I, T, ϵ_N, and V_Q) accordingly. These four parameters are fed into a computer program (EQENV) which integrates the envelope equations and searches for a matched beam (periodic) envelope in the transport section. The injected beam (axisymmetric) has to be transformed into the matched beam (astigmatic) as it passes through the matching section. Another computer code (PARAX) is used to search for the correct voltage settings of four of the five matching quadrupoles . The remaining quadrupole (usually the first or the last one) is set at a fixed voltage.

At the first trial of matching, the mismatch is usually large ($\pm$ 10% variation of the radius as a function of z), but the median radius around which the envelope oscillates is observed to have the same value as the matched radius predicted by the rms envelope equation, within the experimental errors of measuring V_Q, I, T, a, and b. The envelope is insensitive to ϵ_N in the space charge dominated region. The envelope oscillation is measured by monitoring the horizontal and vertical beam profiles in between quadrupoles at various locations in the transport section. Satisfactory matching requires a number of iterations. It is possible to make small corrections by using the calculated 4 x 4 linear response matrix which relates changes of the four matching quadrupole voltages to changes in the envelope parameters (a, a', b, b') at the end of the matching section.

Experimental Results

We investigated to what accuracy we can control the beam radius. For each of the matched beams, we measured the beam radii (squared) at various locations along the focusing channel and compared them with the theoretically calculated value for the equivalent K-V beam. The results are summarized in Fig. 2 for $\sigma_0 = 60°$. The errors indicated by the circles correspond to the amplitude of the envelope oscillation and the measurement errors of ϵ_N. The measurement errors of the beam radii are much smaller than the amplitude of the envelope oscillation. The phase shifts (σ) are also calculated values for the equivalent K-V beams and range from 12° to

55° as indicated in Fig. 2. We are in the process of modifying the injector to achieve even greater tune depression (down to approximately 6°). Values of σ_0 have been varied from 45° to 120°.

The effect of nonlinearities is studied by monitoring the distortions of the particle distribution (usually the figure-S shape). The effects are undetectable for the largest beam radius we have studied so far. The largest matched beam radius was 15.5 mm between the quadrupoles and 19 mm (inferred) in the middle of the focussing lens. This corresponds to more than 80% of the bore radius (25.4 mm) when the mismatch oscillations (±5% of the radius) and the equilibrium orbit errors (±2 mm) are taken into account.
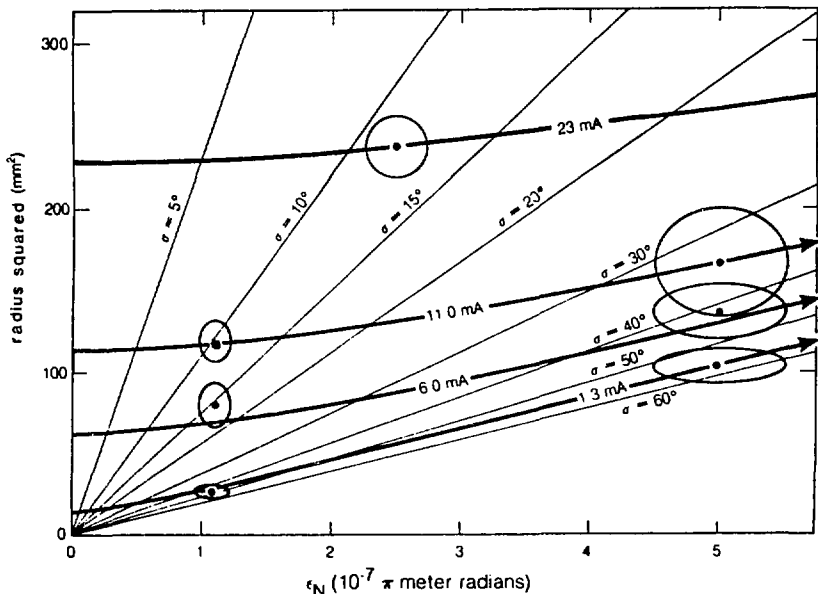
Fig. 2. Experimental matched beam radii (squared) for various emittances and currents in a $\sigma_0 = 60°$ lattice. The values of σ are calculated and the currents used experimentally are fitted for the equivalent K-V beam which has the same total current, but has $\epsilon_N = 4\ \epsilon_{rms}$ and has a radius = 2 x_{rms}. Approximate errors for ϵ_N and the amplitudes of the mismatch oscillation are indicated with an ellipse for each data points.

The particle distribution function at the injector is semi-Gaussian with an elliptical current profile projected in either the x or y directions as mentioned earlier. The distribution functions measured at the end of the transport section appear to be different qualitatively depending on the degree of tune depression as well as on the stability of the beam. These differences are illustrated in Fig. 3a, b, c for $\sigma/\sigma_0 = 12°/60°$ (stable), $50°/60°$ (stable), and $36°/120°$ (unstable). For $12°/60°$, the semi-Gaussian nature of the distribution is approximately preserved with the exception that there is a slight flattening tendency of the otherwise elliptical current profile (Fig. 3a). The flattening may mean hollowing of the current density distribution (j vs. x and y) on the beam axis by approximately 10%. For $50°/60°$, the observed distribution appears to be a full-Gaussian (Fig. 3b), i.e., Gaussian in both configuration and velocity space. A typical distribution after it has gone through an instability is shown in Fig. 3c. Dangerous instabilities such as this cause an irregular beam profile, a halo around the beam, and a significant current loss. The remaining beam has a much larger emittance than the injected beam.

The semi-Gaussian distribution is a self-consistent one for a focussing channel which has a cylindrical square-well potential, in the sense that the form of the distribution function does not change along the channel. In the present experiment, a focussing field somewhat similar to the square-well shape is formed for $(\sigma/\sigma_0)^2 \ll 1$ because the average focussing field inside the beam is reduced by the space charge of the beam by a factor $(\sigma/\sigma_0)^2$ while the reduction outside of the beam decreases as $1/x$.[9]

For each of the matched beams, we measured the emittance, size, and current at the beginning and at the end of the transport section: the beam is inferred to be stable if these values do not change within the experimental error. The results are summarized in Fig. 4 as the stable and unstable regions in the j vs. (σ/σ_0) parameter space. The dependence of j on σ/σ_0 is calculated for the K-V distribution for the actual experimental geometry. For $\sigma_0 = 60°$, the dependence agrees very well with the prediction of the smooth approximation.
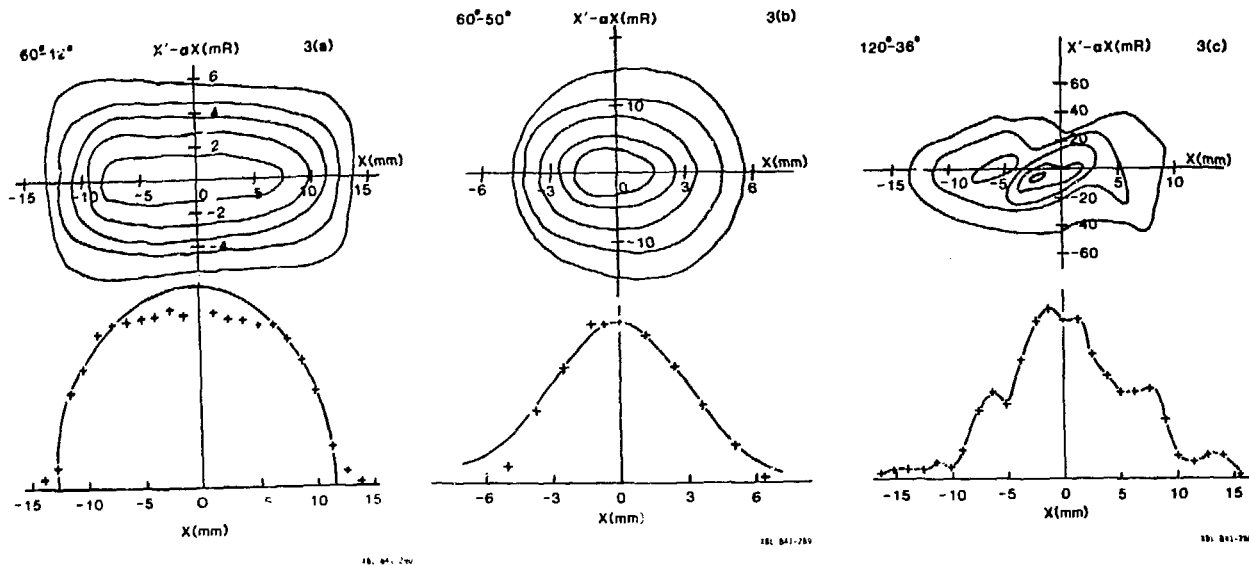
Fig. 3. The particle distribution in the phase space (x' − αx, x) and the current profile (∫jdy vs. x) are shown for the three representative cases. The coordinate transformation x' ⇒ x' − αx suppressed the tilt of the contours for the distribution in the middle of two adjacent quadrupoles. The contours plotted here correspond to 10, 30, 50, 70, and 90% of the peak of the distribution, respectively. (a) A high space charge stable beam case with $\sigma_0 = 60°$ and $\sigma = 12°$, measured at Q80. An elliptical profile is shown for comparison with a semi-Gaussian distribution. (b) A low space charge stable beam case with $\sigma_0 = 60°$ and $\sigma = 50°$, measured at Q80. A Gaussian profile is shown for a comparison with a full-Gaussian distribution. (c) An unstable beam case with an injected current corresponding to $\sigma_0 = 120°$ and $\sigma = 36°$, measured at Q44, where the current was only 60% of the injected value.
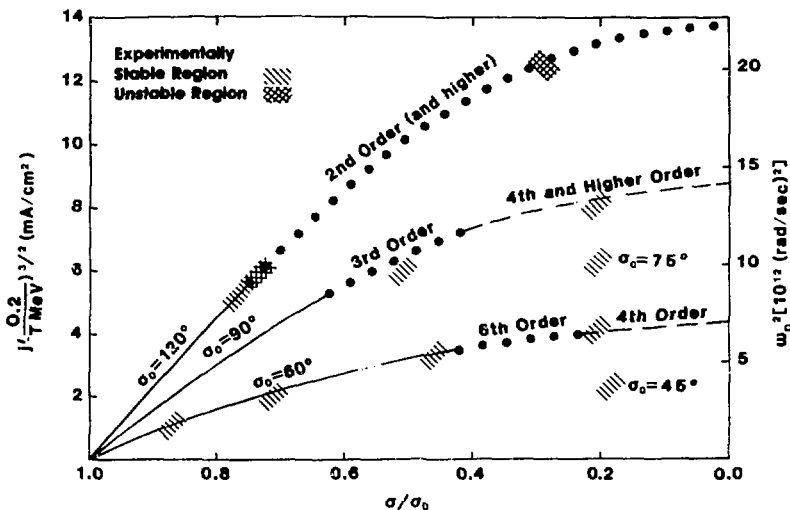
Fig. 4. Experimentally measured stable and unstable regions. Analyti-
cally predicted unstable modes for D-V distribution are shown
for comparison

The stability of the beam for $\sigma/\sigma_0 = 12^\circ/60^\circ$ implies that the earlier
driver designs, which assumed $\sigma/\sigma_0 = 24^\circ/60^\circ$, are rather conservative.
Since $\sigma \propto \epsilon_N/I$, for the same value of ϵ_N and j, twice the current can be
transported: or for the same value of the beam size a beam with half the
emittance can be transporte   Computer simulations show that σ/σ_0 can be
even smaller[10]. We are now in the process of modifying the injector for
$6^\circ/60^\circ$ operation. In contrast to the case of $\sigma_0 = 60^\circ$, strong envelope
instabilities are observed for $\sigma_0 = 120^\circ$, with an emittance growth by a
factor ~ 2 and current losses when $\sigma \leq 90^\circ$.

Since we did not institute any longitudinal focusing, the head and the
tail of the beam are observed to spread out longitudinally, but the main
body of the beam is not affected. This result agrees quantitatively with
the 1-D computer simulation.[11]

Acknowledgments

References

1. D. Keefe, in these proceedings, Session 4.

2. A. W. Maschke, Brookhaven National Lab. Rep., BNL-20297 (1975).

3. I. Hofmann, L. J. Laslett, L. Smith, and I, Haber, Particle Accelerators, 13, 145 (1983).

4. W. Chupp, A. Faltens, E. C. Hartwig, D. Keefe, C. H. Kim, L. J. Laslett, R. Nemetz, C. Pike, S. S. Rosenblum, J. Shiloh, L. Smith, M. Tiefenback, and D. Vanecek, IEEE Trans. Nucl. Sci., NS-30, 2549, (1983).

5. A. W. Maschke, J. Brodowski, and E. Meier, IEEE Trans. Nucl. Sci. NS-30, 2558 (1983).

6. J. Klabunde, M. Reiser, A. Schoenlein, P. Spaedtke, J. Struckmeier, IEEE Trans. Nucl. Sci., NS-30, 2543 (1983).

7. J. D. Lawson, E. Chojnecki, P. Loschialpo, W. Namkung, C. R. Prior, T. C. Randle, D. H. Reading, and M. Reiser, IEEE Trans. Nucl. Sci., NS-30, 2537 (1983).

8. F. J. Sacherer, IEEE Trans. Nucl. Sci., NS-18, 1105 (1971).

9. P. Lapostolle, Proc. VII Int. Conf. on High Energy Accelerators, Yerevan, pp 205-212 (1969).

10. I. Haber, private communication, also in these proceedings, session 5.

11. J. Bisognano, private communication.